

On The Experimental Analysis of the Heating Effect of Open Channel on Thermal and Dynamic Characteristics of the Resulting Flow Plume-Thermosiphon

T. Naffouti^{1, 2, 3, †}, L. Thamri^{1, 4} And J. Zinoubi^{1, 2, 3}

¹ Université Tunis El-Manar, Faculté des Sciences de Tunis, Département de Physique,

² Laboratoire d'Énergétique et des Transferts Thermique et Massique, El Manar 2092, Tunis, Tunisia.

³ Institut Préparatoire aux Etudes d'Ingénieurs El-Manar, El-Manar 2092, Tunis, Tunisia.

⁴ Laboratoire de Mécanique des Fluides et des Transferts Thermique

Corresponding author: T. Naffouti

ABSTRACT: This paper deals with an experimental investigation of the heating effect of a vertical open channel on the behavior of the resulting flow of thermosiphon with thermal plume generated by a hot block localized at the entry of a prallelepipedic channel. The active heater of the plume of rectangular form is maintained at a constant temperature 300 °C only along top wall of the block. Joule effect is used to isothermally heat internal walls of the channel. Consequently, the heating of this one causes the propagation of a thermosiphon flow which interacts with that of plume. A constant current anemometry (CCA) method is adopted to handle the study, which has been conducted for Prandtl number and Grashoff numbers at 0.71 and $0.86 \cdot 10^7$, respectively. Results were reported for different channel heating from 34 to 80 °C. It is concluded that the channel heating is the significant parameter affecting average and turbulent thermal and dynamic fields of the resulting flow. The analysis of average characteristics shows that the interaction between thermal plume and thermosiphon becomes weaker as increasing the channel heating. It is found an enhancement of flow rate and energy absorbed by the fluid with increasing the temperature of channel internal walls. Results of turbulent characteristics of the flow show an attenuation of the turbulence intensity close to top of hot block as increasing the channel heating. The examination of dynamic turbulence rates and transversal repartitions of thermal and dynamic skewness and flatness factors proves a considerable homogenization of fine structure of the resulting flow at the channel exit for higher heating of this one thus indicating the turbulence establishment.

KEYWORDS: thermal plume, thermosiphon flow, interaction, heating channel, average characteristics, turbulent characteristics.

Date of Submission: 18-04-2018

Date of acceptance: 03-05-2018

I. INTRODUCTION

Thermal plume evolving in free and semi-confined/confined environment is one of the preferred solutions to control several problems encountered in nature and industry. This natural convection flow plays a very interesting role in several applications, such as forests fires, environmental pollution, tornado, industrial chimneys thermal exchanger, thermal design of buildings and many others [1-5]. For this reason, a great number of researches related to free thermal plumes or their interactions with neighboring environment are presented.

Various researchers are investigated experimentally and numerically free thermal plumes generated by hot sources of different forms disc/spherical calotte/rectangular block/cylinder/plate... [6-16]. They concluded that average and turbulent fields of the ascending flow are divided in two different zones. Upstream of the heater, a first zone is characterized by significant temperature and velocity. Downstream, a second zone is described by plume lateral expansion where the establishment of thermal and dynamic turbulence of the flow. In this region, it is found that the behavior of free thermal plume is independent of the geometry of hot source just far from of this one. Furthermore, they showed that the flow rate and the heat flux absorbed by the air increase as move away from the active heater.

In reality, the thermal plume interacts with various obstacles which are in the vicinity. So, this flow

kind can be communicated with a semi-confined environment delimited by one or several plan/cylindrical/spherical walls. Literature reviews shows that this interaction is classified mainly in three category; interaction plume-wall, plume-plume and plume-thermosiphon. In order to understanding complexes mechanisms of phenomenons generated by this communication, a small number of investigations are carried out. For example, Y.Jaluria [17] experimentally studied the interaction of a thermal plume with a neighboring vertical surface. It is prove that the flow is strongly deflected towards the surface. After, J.M.Agator [18] performed an experimental investigation on the interaction between vertical plate and a turbulent thermal plume generated by hot spherical calotte. He concluded that the structure of the flow is similar to that of free thermal plume. It is noticed a dissymmetric behavior of thermal and dynamic turbulent fields owing to deviation of the plume axis towards the wall. Thereafter, J.M.Agator [18] examined the interaction of two close identical thermal plumes localized in the vicinity. It is demonstrated an intensification of entrainment phenomenon of fresh air in the region between hot calottes. Using two hot flat discs, M.Brahimi [19, 20] is concentrated on the interaction of two identical thermal plumes evolving in free environment. Results show a strong interference of plumes downstream of active sources. Also, it is concluded that the temperature fluctuations of resulting flow are more sensitive than those of the only plume. E. Moses et al. [21] performed an experimental analysis of the dynamics and interactions of thermal plumes created by a localized heat source. The instantaneous visualization of the resulting flow proves that the interaction of plumes becomes more intense as we move away from heaters.

A.O.M.Mahmoud et al. [22] are focused their investigation on the interaction of a thermal plume with a thermosiphon flow. It is found a detection of a supplementary zone which adds to classical zone of a free plume. This zone is described by the formation of two symmetrical counter-rotating rolls near the hot disc generator of the plume. They concluded an intensification of heat flux absorbed by the air and flow rate inside the cylinder than that of free thermal plume. After, J.Zinoubi et al. [23] investigated effects of geometrical parameters on the behavior of resulting flow plume-thermosiphon into vertical cylinder. It is shown that the structure of the flow is similar to that of free plume for disc-cylinder spacing equal to 6 cm. Experimental results demonstrate that decrease of this spacing conduct to a fast homogenization of fluid at the cylinder exit and an increase of flow rate of the flow. By studying a guided thermal plume by a vertical cylinder, J.Bouslimi et al. [24, 25] observed a lateral expansion of the plume at the cylinder entry. In addition, it is found that evolutions of thermal and dynamic flatness and skewness factors approach a Gaussian law particularly in turbulent regions of the resulting flow. J.Zinoubi et al. [26] examined the interaction of a thermal plume with a thermosiphon flow inside a vertical canal open a tends. For this configuration, the plume is created by an horizontal disc heated at a constant temperature. The analysis of thermal and dynamic field shows the evolution of the resulting flow in three zones. A contraction of the size of counter-rotating rolls is visualized. After that, A.O.M.Mahmoud et al. [27] conducted an experimental study on the influence of different geometrical parameters on thermal and dynamic characteristics of a generator of solar hot air. They noted that the heat flux absorbed by the air and the flow rate of the flow plume-thermosiphon increase for a reduction of the disc-cylinder spacing and the cylinder height. T.Naffouti et al. [28, 29] are interested to thermal plume generated by a rectangular hot obstacle placed at the entry of a prallelepipedic canal. It is concluded that the average and turbulent structures of the plume are affected by the thermosiphon flow. Flow visualization by laser plan and analysis of thermal and dynamic fields show the appearance of a supplementary just above active source characterized by an impenetrable envelope. By studying the effect of aspect ratio of vertical canal on average and turbulent characteristics of a thermal plume, T. Naffouti et al. [30, 31] proved that for largest spacing, flow structure is similar to thermal plume evolving in free medium. Also, it is demonstrated the existence of an optimum aspect ratio of canal characterized by maximum of turbulent parameters governing the resulting flow of plume-thermosiphon.

Literature reviews show that the subject relating to the influence of heating of semi-confined medium on the resulting flow of thermal plume-thermosiphon has not been discussed. For this reason, an experimental investigation is carried out on the effect of various temperatures of vertical channel on the behavior of the resulting flow thermal plume-thermosiphon. At the laboratory, a rectangular hot block heated at a fixed temperature is localized at the entry of a vertical channel heated by joule effect. The present investigation can conduct to better control phenomenons generated by the development of this natural convection in nature and industry.

Nomenclature

b_1	Source width, m
b_2	Channel width, m
D_f	Sensitive wire diameter, m
e	Spacing between channel walls, m

F_{at}	Thermal flatness factor, ($F_{at} = \frac{\overline{T^{14}}}{(\sqrt{T^{12}})^4}$)
F_{ad}	Dynamic flatness factor, ($F_{ad} = \frac{\overline{U^{14}}}{(\sqrt{U^{12}})^4}$)
F_{dt}	Thermal skewness factor, ($F_{dt} = \frac{\overline{T^{13}}}{(\sqrt{T^{12}})^3}$)
F_{dd}	Dynamic skewness factor, ($F_{dd} = \frac{\overline{U^{13}}}{(\sqrt{U^{12}})^3}$)
g	Gravitational acceleration, $m.s^{-2}$
Gr	Grashoff number, ($Gr = \frac{g \beta (T_s - T_a) b_1^3}{\nu^2}$)
I_t	Thermal turbulent intensity of the flow, ($I_t = \frac{\sqrt{\overline{T^{12}}}}{T_s - T_a}$)
I_d	Dynamic turbulent intensity of the flow, ($I_d = \frac{\sqrt{\overline{U^{12}}}}{U}$)
L_2	Channel Height, m
L_1	Source length, m
L_2	Channel length, m
L_f	Length of the sensitive wire, m
Pr	Prandtl number, ($Pr = \frac{\nu}{\chi}$)
T	Average temperature, K
T_a	Temperature of the ambient air, K
T_s	Temperature of the hot source, K
T_p	Temperature of the hot wall of channel, K
T'	Temperature fluctuation, K
T^*	Dimensionless temperature of the flow, ($T^* = \frac{T - T_a}{T_s - T_a}$)
T_p^*	Dimensionless temperature of hot wall of channel, ($T_p^* = \frac{T_p - T_a}{T_s - T_a}$)
U	Vertical average component velocity of the flow, $m.s^{-1}$
U_0	Reference velocity, ($U_0 = \sqrt{g \beta (T_s - T_a) b_1}$), ms^{-1}
U'	Vertical average component velocity fluctuating of the flow, ms^{-1}
U^*	Dimensionless vertical average component velocity of the flow, ($U^* = \frac{U}{U_0}$)
(x,y,z)	Cartesian coordinates
X^*	Dimensionless coordinate, ($X^* = \frac{x}{b_1}$)
Z^*	Dimensionless height, ($Z^* = \frac{z}{L_2}$)

Greek symbols

β	Thermal expansion coefficient, K^{-1}
ν	Kinematic fluid viscosity, $m^2 \cdot s^{-1}$
χ	Thermal diffusivity, $m^2 \cdot s^{-1}$

II. SPECIFICATION OF THE PROBLEM

By reason of the strong dependence of the flow on the surrounding conditions, the apparatus (Fig.1) is placed in a quiet atmosphere inside an independent closed room. Details of the experimental apparatus have been discussed by T.Naffouti et al. [15]. The system is essentially the association of a rectangular block (1) localized at the entry of a vertical channel (2) open at ends. The channel of width $b_2 = 15$ cm and height $L_2 = 40$ cm is constituted by two parallel square Duralumin flats plates and two other rectangular Plexiglas plates. Duralumin walls are heated symmetrically by joule effect at uniform temperature ranging from 34 to 80 °C. The active block generator of thermal plume with length of $L_1 = 40$ cm and width of $b_1 = 6$ cm is heated only at the upper surface by joule effect at 300 °C. The heating of channel with thermal radiation emitted by the block and by joule effect creates an aspiration of a thermosiphon flow which interact with that of plume. The model is fixed on a frame (3) at 80 cm above the ground to allow air supply from below. In order to measure the fluctuations of temperature and velocity of the flow, the technique of a resistant wire anemometer at constant current (CCA) is applied. The available literature shows that several experimental investigations relating to natural convection problems are performed with this technique [18-20, 22-31]. In the present investigation a calibrated hot wire probe (4) is placed inside the channel to communicate with the fluid. The diameter of cylindrical sensitive platinum wire of the probe is $D_f = 7.5 \mu m$ and its length is $L_f = 3$ mm. To move the probe in the x and z directions, displacement system (6) is used. To measure temperature and velocity of the resulting flow, the probe is supplied by a current of 1.2 and 50 mA, respectively. A computer connected with a data acquisition card can save the instantaneous measurements of temperature and velocity fields (5, 7, 8). Shannon theorem is used and the adopted sampling period is 15 ms. Figs.2 and 3 illustrate thermal and dynamic signals detected by the probe inside the channel.

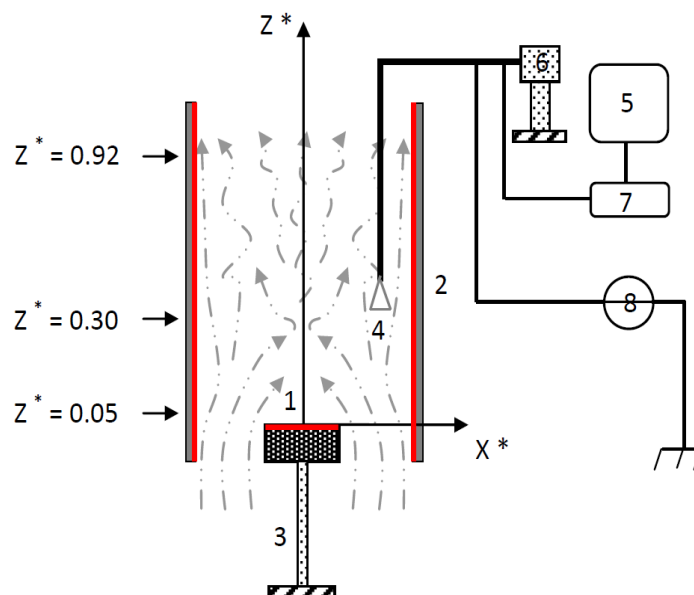


Figure 1 Experimental apparatus and study sections

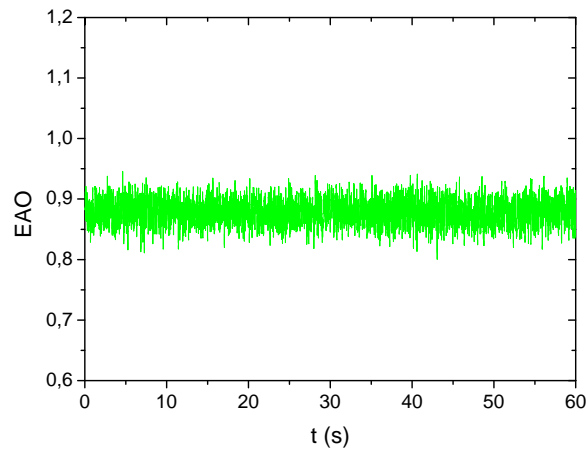


Figure 2 Example of temperature signal delivered by the probe

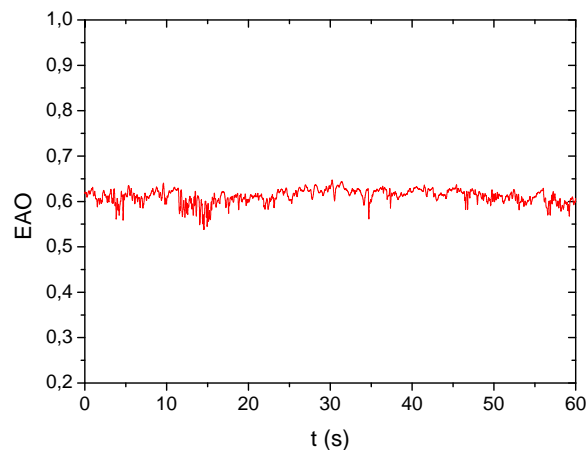


Figure 3 Example of velocity signal delivered by the probe

III. RESULTS AND DISCUSSIONS

Average and turbulent characteristics of the resulting flow for various values of the channel heating are examined in this section. Experimental results are performed for fixed Grashoff number and Prandtl number at $0.85 \cdot 10^7$ and 0.71, respectively. The present problem of 2-D is carried out for three dimensionless heating of internal walls of channel by Joule effect; $T_{p2}^* = 0.084$, $T_{p3}^* = 0.139$, $T_{p4}^* = 0.194$ corresponding to $T_{p2} = 50^\circ\text{C}$, $T_{p3} = 65^\circ\text{C}$, $T_{p4} = 80^\circ\text{C}$. Thus, different parameters governing the flow are presented just on the mid-plane of channel (xOz).

3.1 Heating effect of channel on average characteristics of the resulting flow

3.1.1 Vertical evolution of the dimensionless temperature

On figure 4 is presented the vertical evolution of the dimensionless flow temperature on the mid-median plane of the hot obstacle (yOz) for four channel heating. For heating the channel walls by thermal radiation, corresponding to the temperature T_{p1}^* , the profile is described by three different flow behavior thus indicating the existence of three zones of flow previously reported in the work of T. Naffouti et al. [28, 29]. In the first zone ($z^* < 0.20$) close to the active obstacle, the temperature is more intense owing to dominance of the thermal plume. In the second zone ($0.2 < z^* < 0.5$), an attenuation of temperature is detected due to the penetration of the thermosiphon flow which interacts with the plume. In the third zone ($z^* > 0.5$), the temperature remains constant until the channel exit. Increasing channel heating leads to an increase of the flow temperature on the axis (oz). On the other hand, thermal profiles indicate a variation of the boundaries of three zones of the resulting flow. Near the active

source, the first zone becomes more elongated in the vertical direction as the heating increases. This shows that the plume-thermosiphon interaction becomes weaker with increasing channel heating due to the thermosiphon deflection towards vertical hot walls. Higher up, the second zone is characterized by a considerable attenuation of the temperature with a decrease of this region with the increase of channel heating. At the channel exit, the third zone is characterized by comparable temperatures.

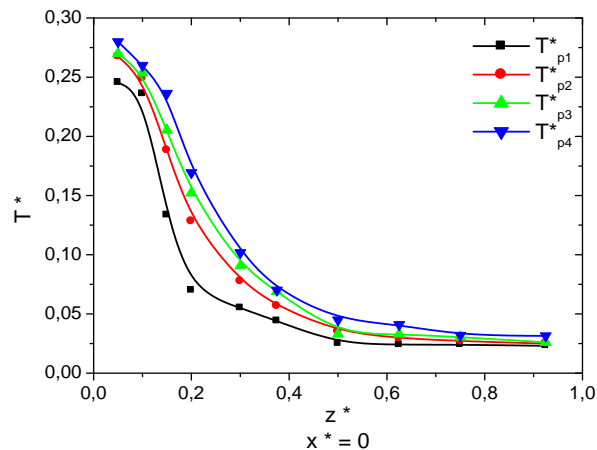


Figure 4 Vertical evolution of the dimensionless temperature of the flow for various heating channel

3.1.2 Transversal distribution of the dimensionless temperature

The transverse distribution of the average dimensionless temperature of the flow for three sections Z^* with different channel heating is illustrated in figure 5. Profiles behavior consolidates the evolution of the flow in three zones for each channel heating. For the case of channel heating of the by thermal radiation T^*_{p1} and in the first section $z^* = 0.05$, thermal gradients are more intense just above the hot block owing to a sudden transformation of the ambient air into thermal plume. On both sides of this block, the temperature is very low due to the existence of the thermosiphon flow which interacts with the plume. A little further up the hot source $z^* = 0.3$, the thermal profile shows a considerable decrease of the temperature in the central region of the resulting flow. Far from the source generating the plume with $z^* = 0.92$, the temperature remains practically constant over the entire upper part of the channel thus reflects the homogenization of the upward flow. By increasing the channel heating, there is also an intensification of the thermal field of the flow from the inlet to outlet of the channel. On the other hand, the resulting flow becomes more homogeneous in the upper region of the channel as the heating of the vertical flat plates thereof decreases.

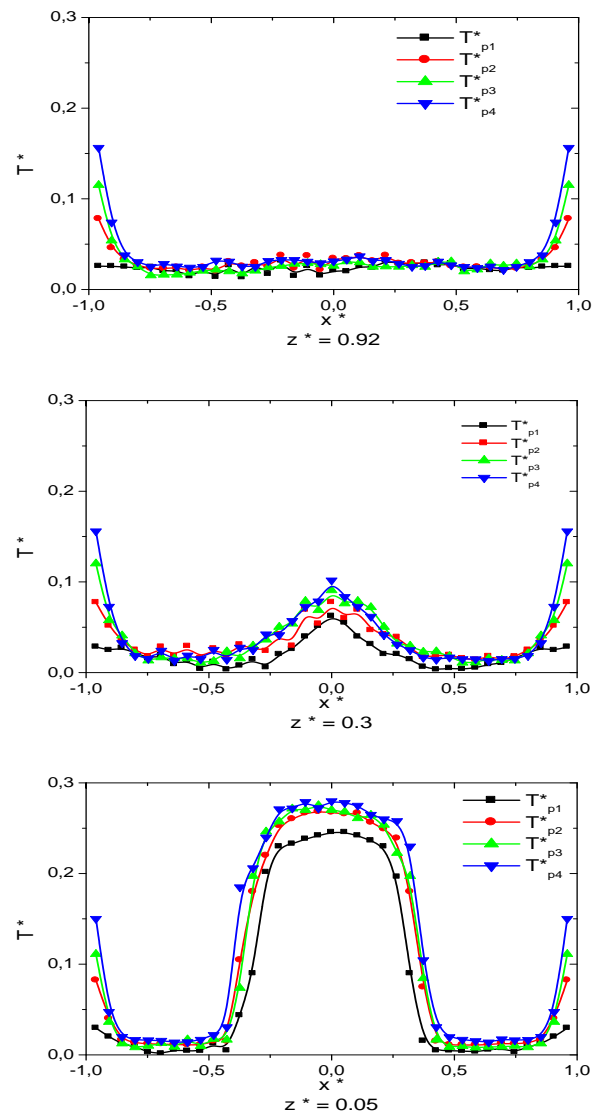


Figure 5 Transversal distribution of the dimensionless temperature of the flow versus heating channel for three sections Z^*

3.1.3 Vertical evolution of the dimensionless vertical component of the average velocity

Figure 6 illustrates the variation of the average vertical component of the dimensionless velocity on the axis (oz) for different channel heating. For the case of the channel heating without Joule effect T^*_{p1} , the corresponding profile presents three different behaviors of the upward flow which consolidates the evolution of this one into three zones. This result is in good agreement with the work of T. Naffouti et al. [28, 29]. In the first zone ($z^* < 0.20$), it is found that the flow velocity is lower owing to the low circulation of this one in the first zone. For the second highest zone of this source ($0.20 < z^* < 0.60$), the velocity increases to reach its maximum at $z^* = 0.35$ corresponding to a contraction of the resulting flow. Then, the velocity decreases indicating the pre-establishment of a new regime at the channel exit. In the third zone ($z^* > 0.60$), the flow velocity remains practically constant. By increasing channel heating, the figure shows an acceleration of the resulting flow on the axis (oz) in the upper zone of the channel due to an intensification of the thermosiphon flow with the increase of the heating of vertical channel walls.

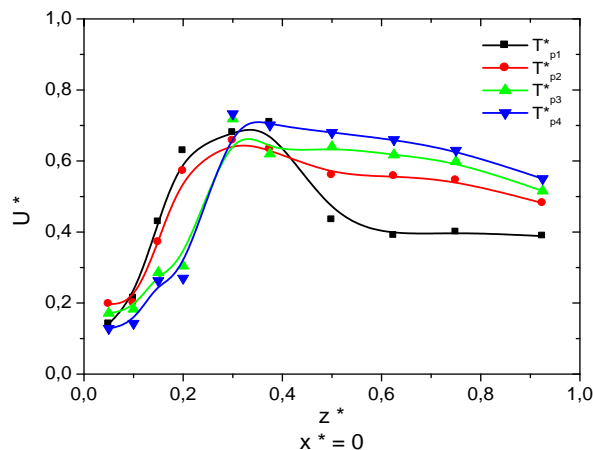


Figure 6 Vertical evolution of the dimensionless vertical component of the average velocity of the flow versus heating channel

3.1.4 Transversal distribution of the dimensionless vertical component of the average velocity

The transverse distribution of the average vertical component of the dimensionless velocity of the flow versus altitude z^* and for different channel heating is illustrated in figure. 7. Profiles consolidate the existence of three zones of the upward flow. For the case where the heating of the plates is done by thermal radiation generated by hot block (T_{p1}^*), results are similar to those of investigations of T. Naffouti et al. [28, 29]. In the first zone near the obstacle $z^* = 0.05$, the dynamic profile shows low velocities just above the block thus proves the existence of a central zone of weak circulation due to the plume blockage by the thermosiphon flow. On the block sides, the velocity is maxima reflecting the existence of an impenetrable envelope formed by the thermosiphon flow. For the second highest zone of the hot source $z^* = 0.3$, the flow becomes more accelerated in the central region of the channel owing to the contraction of the resulting flow. For the section $z^* = 0.92$ of corresponding to third zone, a significant deceleration of the resulting flow with comparable velocities is observed at the channel exit except near the vertical plates thereof. This result shows the establishment of a new regime of flow homogenization at the outlet of the channel. For different channel heating, the structure of the dynamic field is conserved with a change of the height of zones of the flow. For the section $z^* = 0.05$, it is noticed an increase of the flow velocity on block sides with increasing of the channel heating. This proves that the thermosiphon is more accelerated as the channel heating increases. For the section $z^* = 0.3$, the flow becomes more accelerated in the vertical direction due to the attractive effect of hot vertical plates which becomes more intense by increasing the channel heating. This result shows that the interaction between the plume and thermosiphon is weakened with increasing channel heating. For the section $z^* = 0.92$, profiles are almost similar with an acceleration of the flow close to the hot plates of channel.

3.1.5 Vertical evolution of flow rate and the energy absorbed by the fluid

Figures 8 and 9 show the vertical evolution of the dimensionless flow rate Qv^* and the energy absorbed by the fluid H^* for four heating channel. For the case of channel heating by thermal radiation emitted by hot obstacle T_{p1}^* , profiles confirm the results of T. Naffouti et al. [28, 29]. Near the block, the variation of these two parameters is due to an overestimation of the velocity by the probe which can not differentiate between different directions of flow propagation. Far from the active block, profiles show a conservation of the flow rate and the energy until the channel exit whatever the channel heating. On the other hand, figures show a significant enhancement of these quantities owing to the acceleration of the thermosiphon flow and the intensification of the thermal field as the channel heating increases.

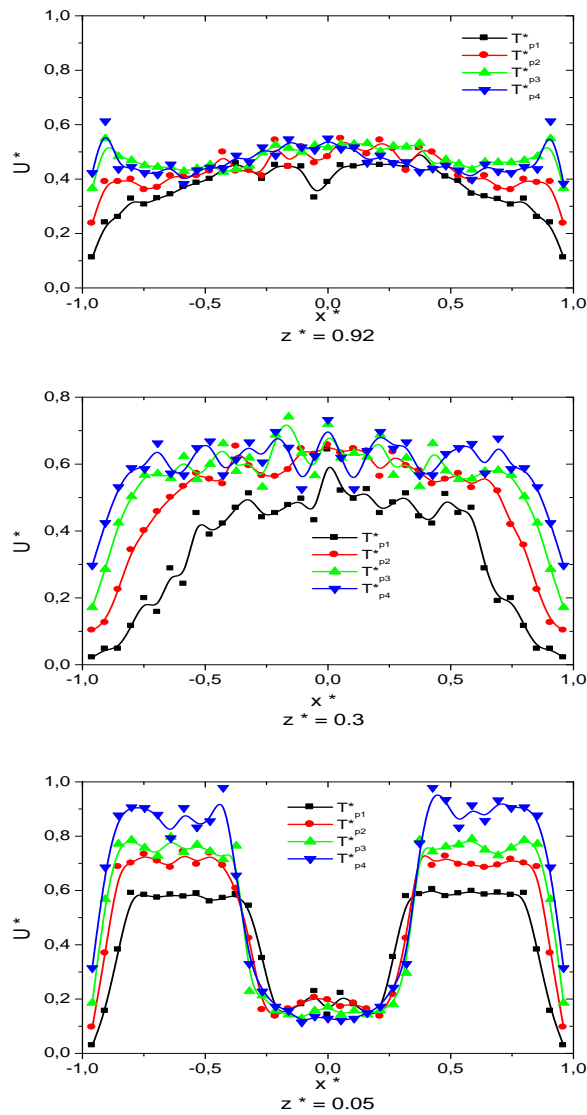


Figure 7 Transversal distribution of the dimensionless vertical component of the average velocity of the flow versus heating channel for three section Z^*

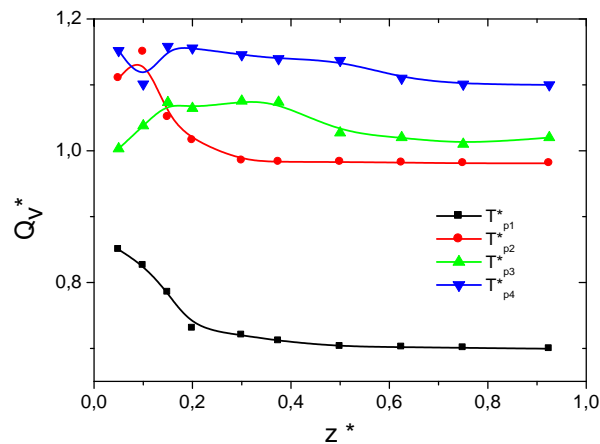


Figure 8 Vertical evolution of flow rate versus heating channel

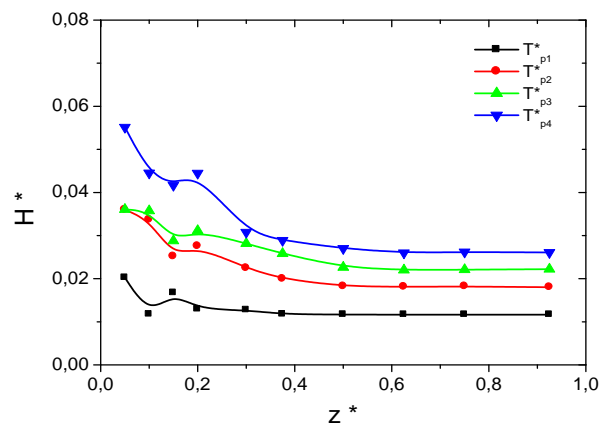


Figure 9 Vertical evolution of energy absorbed by the fluid versus heating channel

3.2 Heating effect of channel on turbulent characteristics of the resulting flow

3.2.1 Transversal distribution of thermal turbulence intensity

On figure 10 is depicted the transverse distribution of the thermal turbulence intensity for three sections z^* and for different channel heating. For case of channel heating by thermal radiation T^*_{p1} , profiles show three different behaviors inside the channel. This observation confirms the evolution of the turbulent thermal field of the flow resulting in three distinct zones. For the first zone in the vicinity of the hot block ($z^* = 0.05$), the corresponding profile shows three extremum of the turbulence intensity. The minimum turbulence about 4.8% reflects a weak interaction between the plume and the thermosiphon on the middle of the median plane (yo_z). Two turbulence peaks about 5.3% are associated with a strong interaction of the thermosiphon with the plume near the axis (oz). On block sides, the turbulence intensity is very low due to the dominance of the fresh air coming from the bottom. For the second highest zone of the block ($z^* = 0.3$), the behavior of the profile becomes more accentuated on the axis (oz) indicating the pre-establishment of a new turbulence regime. For the third zone near the channel exit ($z^* = 0.92$), turbulence rates are comparable about 3.8% over the entire corresponding section which proves the establishment of turbulence. For different channel heating, the turbulent thermal field evolves in three zones with a slight variation of the turbulence rates in the central region of the flow for $z^* = 0.05$ and $z^* = 0.3$. For the section $z^* = 0.05$, increasing the heating channel leads to a low attenuation of the turbulence rates just above the hot block owing to weak interaction of the thermosiphon with the plume. For the section $z^* = 0.3$, the intensity of the thermal turbulence increases on the axis (oz) with the channel heating. For higher section $z^* = 0.92$, profiles are similar for different channel heating.

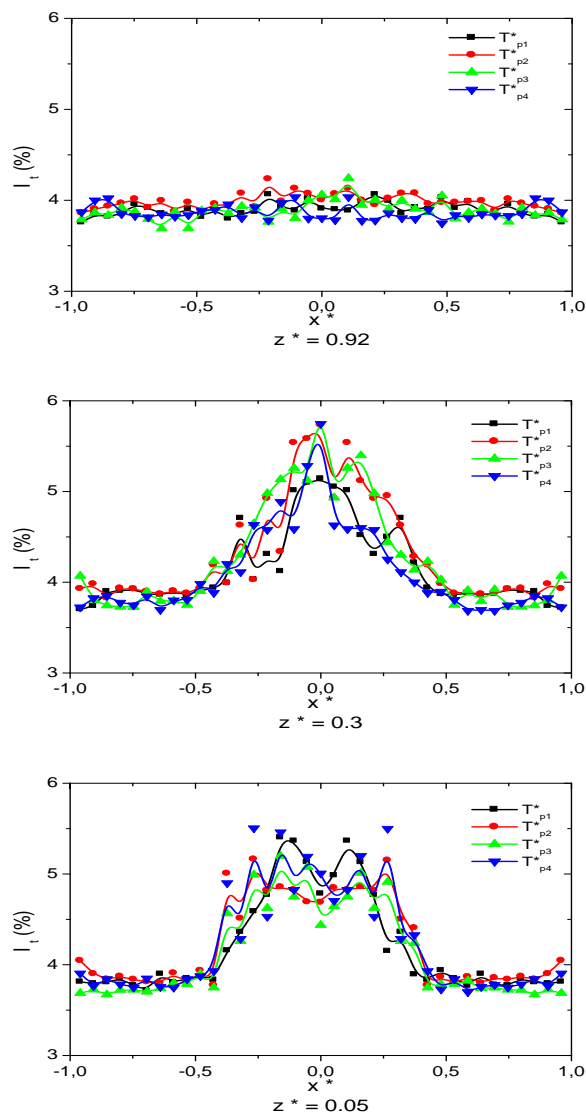


Figure 10 Transversal distribution of thermal turbulence intensity of the flow versus heating channel for three sections Z^*

3.2.2 Transversal distribution of thermal skewness and flatness factor

Profiles relating to transversal distributions of thermal skewness and flatness factors are given in figures 11 and 12 versus various channel heating for three sections z^* . For different channel heating, figures consolidate the evolution of the flow in three zones. For heating by thermal radiation T^*_{p1} , the corresponding profile of the altitude $z^* = 0.05$ of the first zone shows positive values around the axis (oz) due to the preponderance of the thermal plume. On the same axis, the negative dissymmetry proves the penetration of the fresh air from the top of the impenetrable envelope in order to supply the plume from above. In this zone (Figure 12.a), the high values of the flatness factor on either side of the axis (oz) show the existence of the intermittent boundary phenomenon between the plume and the fresh air sucked from below. For the profile corresponding to the section $z^* = 0.3$ located in the second zone (Figure 11), an intensification of different factors is observed on the sides of the active block due to the vertical escape of puffs of hot air. For the section $z^* = 0.92$ of the third zone (Figure 11), the skewness factor is virtually zero over the entire upper part of the channel thus indicates the equiprobability of presence of fresh air and hot air. This observation proves the homogenization of the turbulent thermal field of the resulting flow at the channel exit. In this last zone (Figure 12), the flatness factor is almost equal to 3 which shows that the probability law governing temperature fluctuations is close to the ideal Gaussian law. On the other hand, the increase of heating channel conducts to increase skewness factor especially above the hot block. This result shows the dominance of positive thermal fluctuations related to hot air puffs displaced by the plume to a lower temperature region.

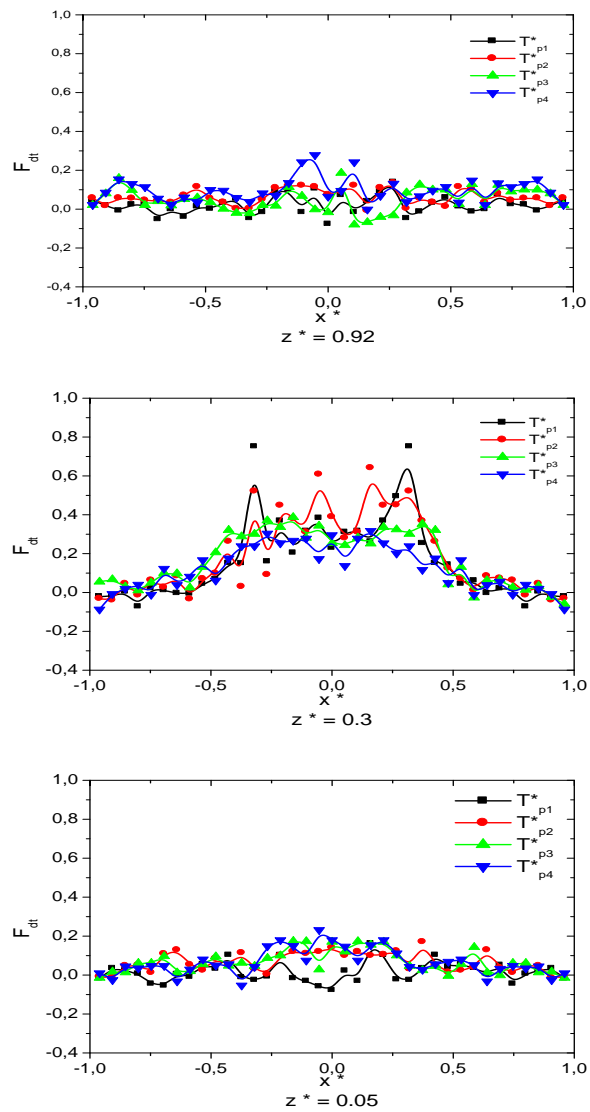


Figure 11 Transversal distribution of thermal skewness factor of the flow versus heating channel for three sections Z^*

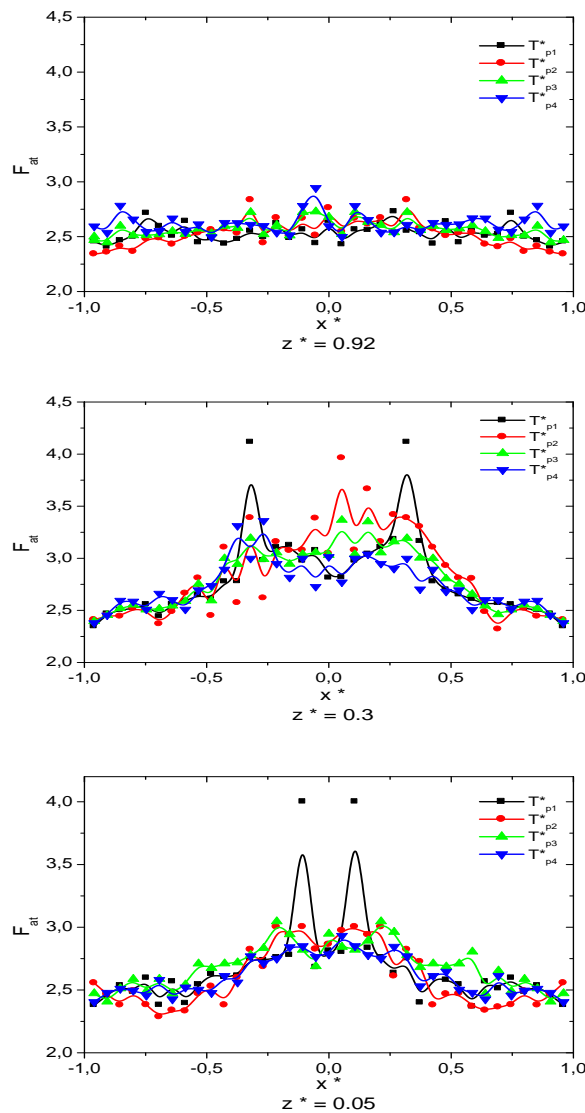


Figure 12 Transversal distribution of thermal flatness factor of the flow versus heating channel for three sections Z^*

3.2.3 Transversal distribution of dynamic turbulence intensity

The transverse distribution of the dynamic turbulence intensity for three sections z^* and for different channel heating is given in figure 13. For channel heating by thermal radiation (T_{p1}^*), profiles show that three different behaviors are in good agreement with the results of T.Naffouti et al. [28, 29]. In the first zone ($z^* = 0.05$), the corresponding profile shows the existence of three extrema above the hot block. Maximum of turbulence rates on either side of the median plane (yOz) reflect the existence of an intense velocity flow of the thermosiphon which envelops the thermal plume. On the axis (oz), the minimum turbulence proves a weak circulation of the plume in the central region of the flow owing to the blocking this one by the impenetrable envelope. In the second zone and for the section $z^* = 0.3$, it is found a decrease of turbulence rates in the central part of the flow which indicates the pre-establishment of a new regime. Near vertical hot walls, the turbulence intensity is more intense due to the movement of the fluid thread which is sometimes attracted by the central flow and sometimes by the wall to continue its way upwards. For the section $z^* = 0.92$ in third zone, the turbulence stabilizes in the central region of the resulting flow indicating the establishment of the turbulent regime. For the other heating T_{p2}^* , T_{p3}^* and T_{p4}^* , the figure shows three different behaviors of the flow inside the channel with a considerable change of turbulence rates near vertical hot walls in particular for the sections of second and third zones. For the first section $z^* = 0.05$, profiles show practically the same evolution except a slight decrease of the dynamic turbulence intensity is observed just above the block. For section $z^* = 0.3$ and in

the vicinity of vertical hot plates (Figure 13), turbulence rates decrease about 42% as channel heating increases. In the upper part of the channel $z^* = 0.92$, profiles become flatter when increasing the heating of the plates thereof. This result proves that the dynamic fluctuating field of the resulting flow becomes more homogeneous for an increase of the channel heating.

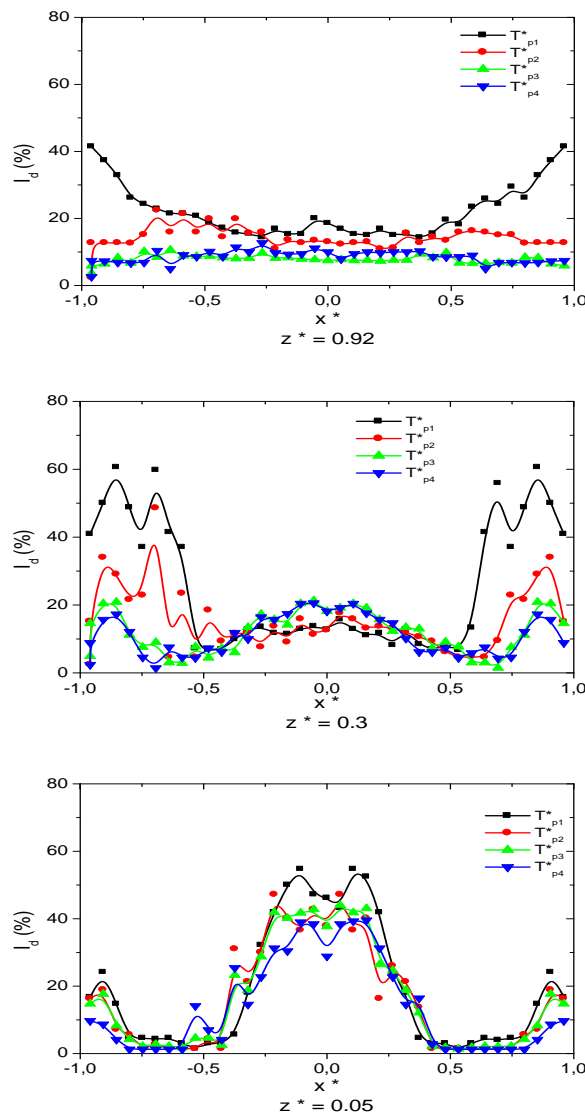


Figure 13 Transversal distribution of dynamic turbulence intensity of the flow versus heating channel for three sections Z^*

3.2.4 Transversal distribution of dynamic skewness and flatness factor

On figures 14 and 15 are illustrated the transverse distributions of dynamic skewness and flatness factors as a function of the channel heating for three sections z^* . For the configuration where the internal walls of the channel are heated by thermal radiation and for section $z^* = 0.05$, the negative skewness just above the hot block proves the existence of a region of weak circulation of the plume. This result is also consolidated by the evolution of the flatness factor which is close to the value 3. In the intermediate region between the block and the channel plates, the positive skewness characterizes the presence of positive fluctuations induced by the thermosiphon flow of high velocity which interacts with that of the plume. For section $z^* = 0.3$, Figure 14 shows an increase of the skewness factor except near the channel plates. In this region, Figure 15 shows maximums of the flatness factor owing to the existence of boundary intermittency at the edges of the hot block between the thermosiphon and the zone of weak circulation. In the upper section of the channel $z^* = 0.92$, skewness and flatness become close to zero and to 3, respectively. This, it proves the establishment of the

turbulence at the outlet of the channel. By varying the channel heating, it is noted that the profiles of the skewness factor have practically the same behavior for each section z^* while the flatness factor is affected in particular for the intermediate section $z^* = 0.3$. In this section, figure 15 shows a significant increase of the dynamic flatness factor as a function of heating channel.

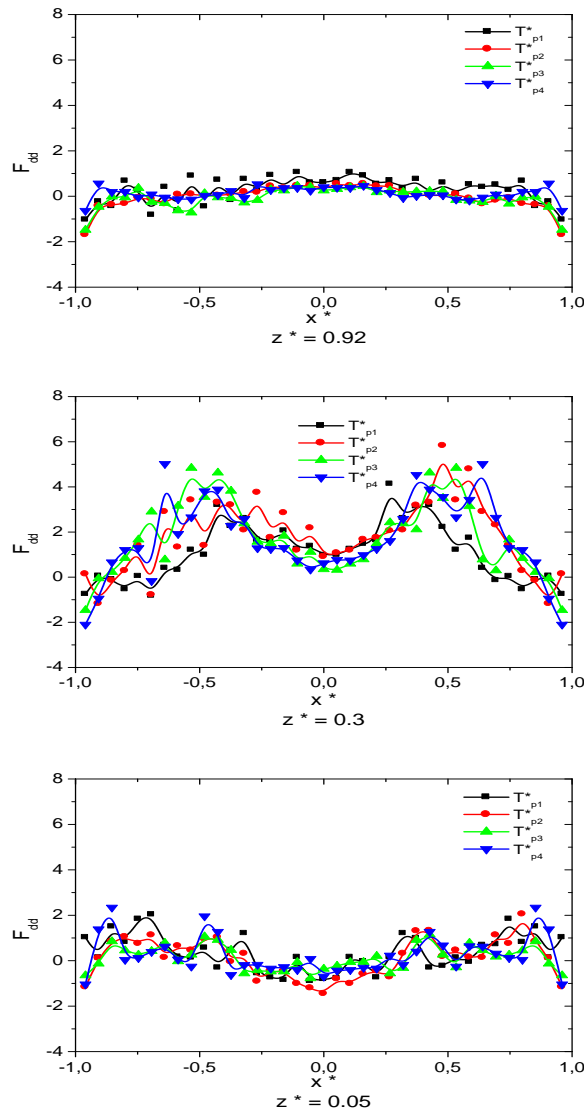


Figure 14 Transversal distribution of dynamic skewness factor of the flow versus heating channel for three sections Z^*

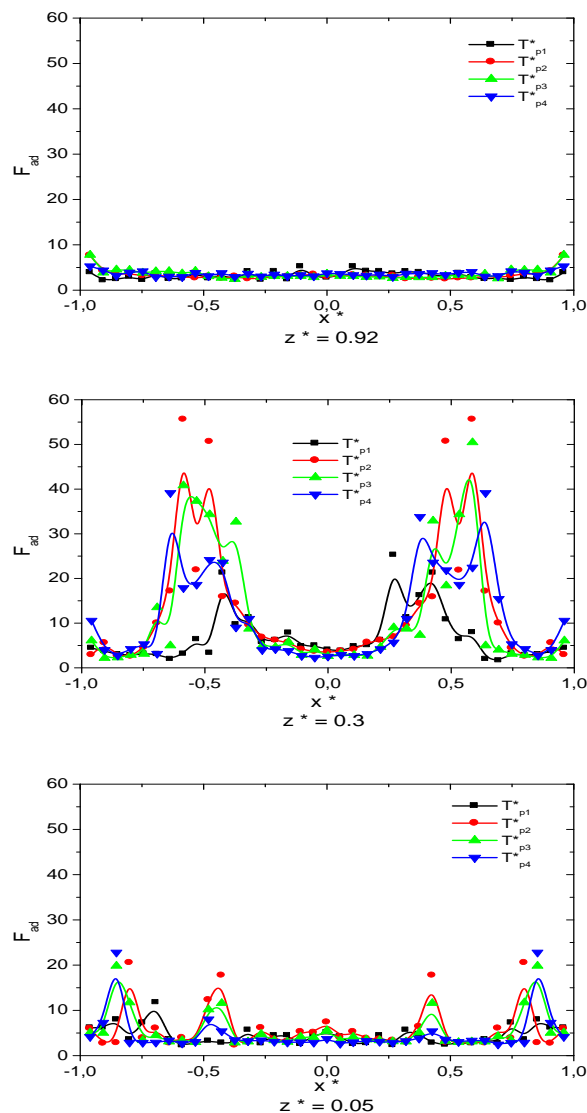


Figure 15 Transversal distribution of dynamic skewness factor of the flow versus heating channel for three sections Z^*

IV. CONCLUDING REMARKS

From experimental results, it can be concluded as follows:

- For different heating of channel, the average structure of the resulting flow is subdivided into three zones. Just above the active source, a first zone ($z^* = 0.05$) described by an impenetrable envelope that prevents the supply of the source from below. Higher, an intermediate zone ($z^* = 0.3$) of flow contraction followed by a third zone ($z^* = 0.92$) characterized by comparable values of velocity and temperature due to the homogenization of the resulting flow at channel exit.

- Increasing of the temperature of channel walls conduct to intensification of the average thermal field.

- Average velocity profiles show that the thermosiphon becomes more accelerated in first zone of the flow by increasing the channel heating.

- In second zone, the study of the transverse distribution of the average vertical component of velocity shows the attractive effect of hot walls of the canal.

- In third zone, the thermal field becomes more homogeneous for a decrease of channel heating due to an intensification of the interaction plume and thermosiphon flows at the entrance of this one.

- The increase of channel heating leads to an improvement of flow rate and the energy absorbed by the fluid owing to the intensification of the thermosiphon which accelerates the upward flow and promotes the transfer of energy from a region at another lower temperature.

- In the first zone, the increase of channel heating conducts to a low attenuation of thermal and dynamic turbulence rates just above the hot block.
- In the intermediate zone, the dynamic turbulence rates are more intense near channel walls as the heating decreases.
- In the upper part of the channel, thermal turbulence profiles are similar and the turbulence intensity remains practically constant over the entire upper section of the channel for different heating. In this region, the dynamic turbulence intensity becomes more homogeneous as the channel heating is increased.
- An increase of the thermal skewness factor is observed just above the active block by increasing channel heating due to an intensification of positive fluctuations generated by the plume in first zone of the flow. In second zone, a remarkable increase of the dynamic flatness factor is observed, on the block sides with channel heating. In third zone, different factors approach the ideal Gaussian law at the channel exit where the establishment of turbulence.

REFERENCES BIBLIOGRAPHIC

- [1] Junmei Li Yanfeng Li Wan Ki Chow Huairong Huang, Numerical studies on fire-induced thermal plumes, *Journal of Thermal Science*, 2005, V 14, Issue 4, pp 374–381.
- [2] Alexander Lavrov, Andrei B.Utkin, RuiVilar, Armando Fernandes, Evaluation of smoke dispersion from forest fire plumes using lidar experiments and modeling, *International Journal of Thermal Sciences*, Volume 45, Issue 9, 2006, pp: 848-859.
- [3] Nelson Molina-Giraldo, PeterBayer, PhilippBlum, Evaluating the influence of thermal dispersion on temperature plumes from geothermal systems using analytical solutions, *International Journal of Thermal Sciences*, V 50, Issue 7, 2011, pp: 1223-1231.
- [4] M. MarroEmail author, P. Salizzoni, F. X. Cierco, I. Korsakissok, E. Danzi, L. Soulhac, Plume rise and spread in buoyant releases from elevated sources in the lower atmosphere, *Environmental Fluid Mechanics*, 2014, V 14, Issue 1, pp 201–219.
- [5] Yan Fu Wang, Pei NaYan, Biao Zhang, Jun Cheng Jiang, Thermal buoyant smoke back-layering length in a naturally ventilated tunnel with vertical shafts, *Applied Thermal Engineering*, V 93, 2016, pp: 947-957.
- [6] B.Guillou, Etude Théorique du développement d'un panache thermique à symétrie axiale influence des propriétés thermophysiques du fluide *Int. Comm. Heat Mass Transfer* Vol. 10, pp. 101-109, (1983).
- [7] H.Q.Yang, Buckling of a thermal plume, *Int. J. Heat Mass Transfer*, Vol. 35, No. 6, pp. 1527-1532, (1992).
- [8] L.Dehmani, Doan Kim-Son, and L. Gbahoué, Turbulent structure of an axisymmetric plume penetrating a strong density stratification, *Int. J. Heat and Fluid Flow*, Vol 17, pp: 452-459, (1996).
- [9] Christian Inard, Amina Meslem, Patrick Depecker, Pierre Barles, Structure moyenne et analyse intégrale du panache thermique des convecteurs électriques, *Rev Gén Therm* Vol 36, pp : 495-509, (1997).
- [10] Leïla Dehmani, Mohamed Maalej, Investigation of the self-similarity of a turbulent plume evolving in a stratified medium, *International Journal of Thermal Sciences*, Vol 41, pp : 773–785, (2002).
- [11] Tetsu Haraa, Shinsuke Katob, Numerical simulation of thermal plumes in free space using the standard ϵ - k model, *Fire Safety*, vol 39 pp 105–129 (2004).
- [12] Minh Vuong Pham, Frédéric Plourde, Son Doan Kim, Effect of swirl on pure turbulent thermal plume development, *International Journal of Heat and Fluid Flow*, Vol 27, pp 502–513, (2006).
- [13] Abdelhakim Bouzinaoui, René Devienne, Jean Raymond Fontaine, An experimental study of the thermal plume developed above a finite cylindrical heat source to validate the point source model, *Experimental Thermal and Fluid Science*, Vol 31, pp: 649–659, (2007).
- [14] Ahmedou Ould Mohamed Mahmoud, Jamel Bouslimi, Rejeb Ben Maad, Experimental study of the effects of a thermal plume entrainment mode on the flow structure: Application to fire, *Fire Safety Journal*, Vol 44 pp 475-486 (2009).
- [15] Taoufik Naffouti, Jamil Zinoubi, Rejeb Ben Maad, Experimental characterization of a free thermal plume and in interaction with its material environment, *Applied Thermal Engineering*, vol 30 pp 1632-1643 (2010).
- [16] Jamil Zinoubi, Taoufik Naffouti, Rejeb Ben Maad, Temperature Spectra from a Turbulent Free Thermal Plume and in Interaction with its Material Environment, *Journal of Applied Fluid Mechanics*, Vol. 4 pp. 69-76 (2011).
- [17] Y.Jaluria ,Thermal plume interaction with vertical surfaces, *Letters in Heat and Mass Transfer* Volume 9, Issue 2, 1982, Pages 107-117.
- [18] J.M.Agator, Contribution à l'étude de la structure turbulente d'un panache thermique à symétrie axiale. Interaction du panache avec son environnement limité, Thèse de Docteur-Ingénieur, Université de Poitiers (1983).
- [19] M.Brahimi, Structure turbulente des panaches thermiques, Interaction, Thèse de Docteur en Physique, Université de Poitiers (1987).
- [20] M.Brahimi, L.Dehmani et Doan-Kim-Son, Structure turbulente de écoulement d'interaction de deux panaches thermiques, Vol. 32, No. 8, pp. 1551-1559, (1989).
- [21] E. Moses, G. Zocchi, I. Procaccia and A. Libchaber The Dynamics and Interaction of Laminar Thermal Plumes, *Europhysics Letters*, 14-(1)) pp. 55-60 (1991)
- [22] Ahmedou Ould Mohamed Mahmoud, Rejeb Ben Maad, Ali Belghith, Interaction of a thermosiphon flow with an axisymmetric thermal plume: an experimental study, *Revue Générale de Thermique*, V 37, Issue 5, 1998, pp: 385-396.
- [23] J.Zinoubi, Etude de l'interaction d'un écoulement de thermosiphon avec un panache thermique à symétrie axiale : Influence des paramètres de formes, Thèse de Doctorat, Faculté des sciences de Tunis, (2003).
- [24] Jamel Bouslimi, Etude de la structure turbulente d'un panache thermique se développant à l'intérieur d'un cylindre vertical, Thèse de Doctorat, Faculté des sciences de Tunis, (2005).
- [25] J.Bouslimi, L.Dehmani, Experimental investigation of the thermal field of a turbulent plume guided by a cylinder – preliminary results, *Experimental Thermal and Fluid Science* Vol 29, pp: 477–484, (2005).
- [26] Jamil Zinoubi, Adel Gammoudi, Taoufik Naffouti, Rejeb Ben Maad, and Ali Belghith, Développement of an Axisymmetric Thermal Plume between Vertical Plates, *American Journal of Applied Sciences* 4 (9): pp 697-685, (2007).
- [27] Ahmedou Ould Mohamed Mahmoud, Jamil Zinoubi, Rejeb Ben Maad, Study of hot air generator with quasi-uniform temperature using concentrated solar radiation: Influence of the shape parameters, *Renewable Energy*, Vol 32, pp: 351–364 (2007).

- [28] Taoufik Naffouti, Mahmoud Hammami, Mourad Rebay and Rejeb Ben Maad, Experimental study of a thermal plume evolving in a confined environment: Application to fires problems, *Journal of Applied Fluid Mechanics JAFM*, May, 2 (1): pp 29-38, (2009).
- [29] Taoufik Naffouti, Jamil Zinoubi and Rejeb Ben Maad, Experimental characterization of a free thermal plume and in interaction with its material environment, *Applied Thermal Engineering*, 30 (13): pp 1632-1643, (2010).
- [30] Taoufik Naffouti, Jamil Zinoubi and Rejeb Ben Maad, Experimental Investigation of the Effect of Spacing between Vertical Plates on the Development of a Thermal Plume from an Active Block, *Journal of Applied Fluid Mechanics* 8 (1): pp 75-84, (2015).
- [31] Taoufik Naffouti, Jamil Zinoubi and Rejeb Ben Maad, On the effect of aspect ratio of open heated canal including an active obstacle upon the turbulent characteristics of a thermal plume: experimental analysis, *Journal of Applied Fluid Mechanics* Vol. 9, No. 6, pp: 3061-3071 (2016).

T. Naffouti "On The Experimental Analysis of the Heating Effect of Open Channel on Thermal and Dynamic Characteristics of the Resulting Flow Plume-Thermo siphon" *American Journal of Engineering Research (AJER)*, vol. 7, no. 5, 2018, pp.89-106.